Seismic analysis of Pine Flat concrete dam

Seismic Analysis of PINE FLAT Concrete Dam

Dam-Reservoir-Foundation System Dynamic Response of PINE FLAT Concrete Dam

Valente S.[1], He Q.[2] and Capriulo C.[1]

[1] *Department of Structural, Geotechnical and Building Engineering, Politecnico di Torino, Italy*

[2] *College of Water Conservancy and Hydropower Engineering, Hohai University, China*

E-mail: silvio.valente@polito.it

ABSTRACT: Investigating the dynamic response of a concrete gravity dam (Pine Flat) is the objective of this study. The acoustic-structure coupling interaction is applied to simulate the reservoir-dam system. The effect of foundation size and the efficiency of the infinite element available in the ABAQUS code to model boundaries are studied. From the comparison of displacement, dynamic pressure and acceleration time history, the evaluation of the dam response to the rising water level is performed. The concrete damaged plasticity model is adopted to evaluate the damage and cracking of the dam caused by Taft earthquake.

1 Introduction

This document has to be read together with the formulation document of Theme A of the 15th ICOLD International Benchmark Workshop on Numerical Analysis of Dams [1], containing more details on geometrical and mechanical data, and together with the final document, prepared by the formulators and containing the full set of results obtained by all participants to the benchmark workshop.

Pine Flat Dam, located on King's River, east of Fresno, California (Figure 1), was constructed by the US Army Corps of Engineers in 1954. It consists of thirty-six 15.25 m-wide and one 12.2 m-wide monoliths. The length of the straight gravity dam is 561 m and the tallest non-overflow monolith is 122 m high (Figure 2)

Figure 1: Downstream view of Pine Flat Dam

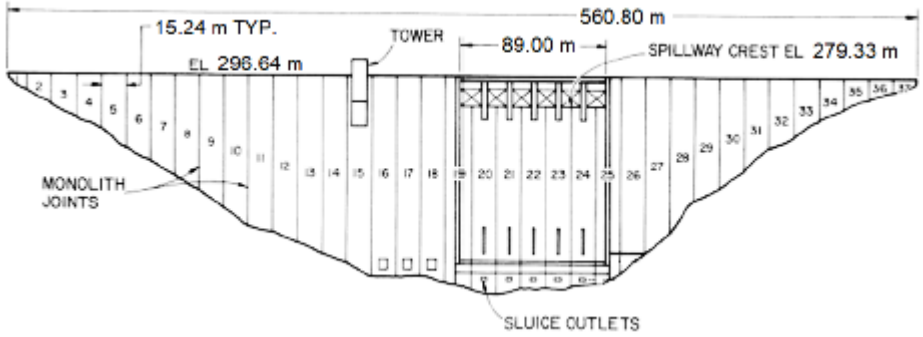

Figure 2: Downstream view of Pine Flat Dam [1]

This study is aimed at identifying key uncertainties that may significantly affect numerical modelling results, at determining the need for future investigations and at developing the best practices in the advanced analysis of concrete dams. This case includes an analysis of the tallest non-overflow dam monolith, no. 16 (Figure 3).

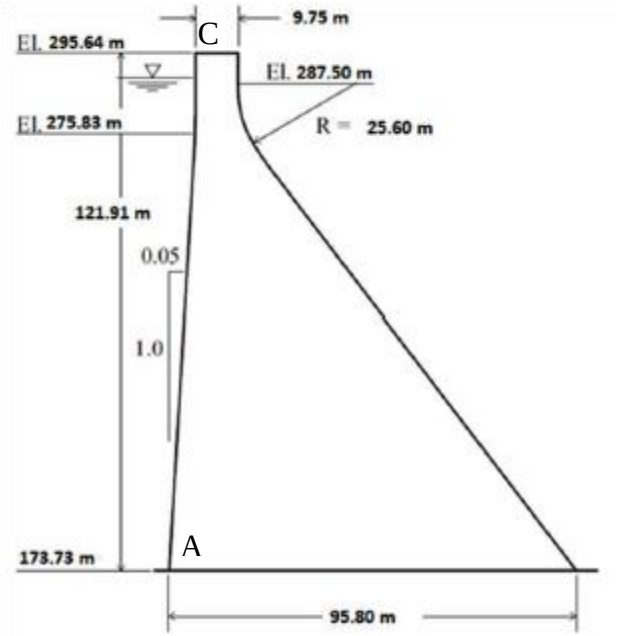

Figure 3: Cross Section Geometry of Monolith 16

2 Method and Approach

All the analyses were carried out by the Finite Element Method (FEM) using the ABAQUS code [2]. The models include the dam monolith 16 , a relevant portion of foundation and of reservoir (complete model), with exception of model B. The mesh, showed in Figure 4, is made of continuous solid, acoustic, and interface elements. The mesh is finer for case B (1x1 m) and case C (1x1.5 m). In case B also a larger foundation length (3700 m) is analyzed.

The reservoir was modelled by acoustic elements, considering the fluid as incompressible. The pressure in the fluid elements accounts for the hydro-dynamic effects only, while hydrostatic pressures were directly applied at the faces where the reservoirs interacts with the dam and the foundation. A boundary condition of zero pressure was applied to the upper surface of the reservoir model.

The dynamic cases were analyzed using an implicit direct integration scheme. The interaction between the dam and the reservoir is achieved through the classic structural-acoustic coupling on the upstream face of the dam, where the normal component of the dam acceleration is proportional to the normal gradient of the water hydrodynamic pressure [3]. The upstream truncation of the reservoir is provided with a non-reflecting acoustic condition.

The only considered static loads are the weight of the dam and of the water (the weight of the foundation is not included in the analysis). The weight of water is applied as hydrostatic pressure on the upstream face of the dam and on the surface of the foundation.

In all cases (A to E) a wave propagation problem in unbounded domain has to be solved. In order to truncate properly the domain analyzed, an artificial boundary condition has to be applied. Such condition is designed so that the outgoing plane waves can correctly cross the external borders of the truncated foundation. In these conditions the normal and tangential stresses are equal to the mass density multiplied by the normal and tangential component of the

velocity respectively. As a consequence, in order to prevent large rigid body motions, a self-equilibrated loading condition has to be applied. Since the self-weight of the dam and the water is not a self-equilibrated condition, in a first step the foundation boundary is assumed as fixed. In a second step, the reaction forces obtained in this way, together with the self-weight, are applied to a model with an artificial viscous boundary. This procedure can reduce the rigid body motions of the model. In any case, when the displacement time history is required, a base line correction in applied.

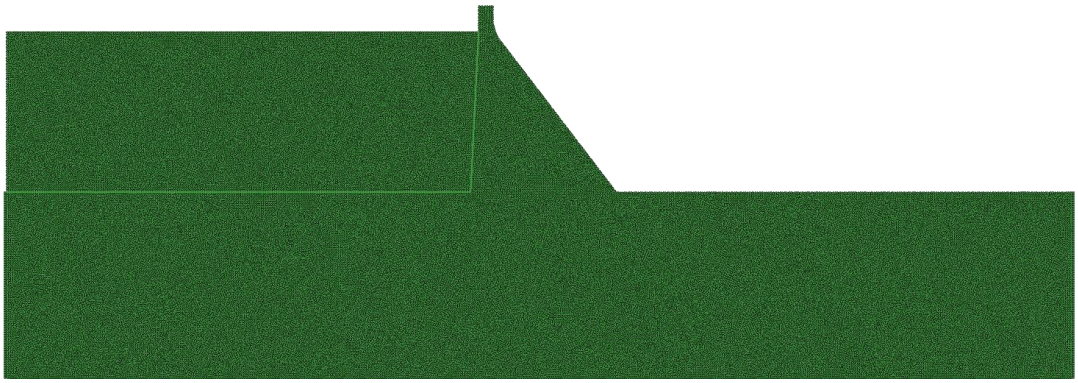

Figure 4: Finite-infinite model of the monolith, the foundation and the reservoir (Element size 1.48×1.48 m)

3 Results

3.1 Case A

Modal analysis was performed both for WRWL (winter reservoir water level) and SRWL (summer reservoir water level). Results are shown in Figure 5. The rise of reservoir water level induces a decrease of the natural frequencies (maximum 7.4% for the second mode, minimum 0.7% for the fifth mode). For this analysis the boundary nodes of the foundation are assumed as fixed.

This model was also excited by an eccentric-mass vibrating generator (EMVG) applied at the dam crest. In this case, in order to allow the propagation of elastic waves to an infinite domain, a viscous artificial boundary is applied at the foundation nodes. It is true that the external force is not self-equilibrated, but it is very small. As a consequence, also the rigid body motion is very small. It is eliminated by a base line correction of the displacement histories. A viscous dumping of 2% was applied to the dam and foundation.

Since in this case a concentrated force is applied to the near-field-domain (see [4]), the infinite elements provided by the Abaqus code have one function only: not reflecting the outgoing waves. This function is performed properly.

The four time histories obtained by the authors (displacement and acceleration at the dam heel and crest) are shown in the complete report prepared by the formulators and are not repeated here.

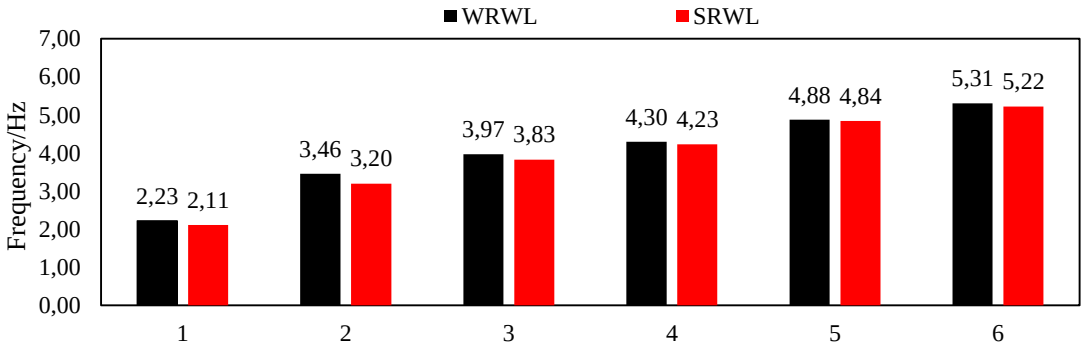

Figure 5: Nature frequency for different reservoir water levels

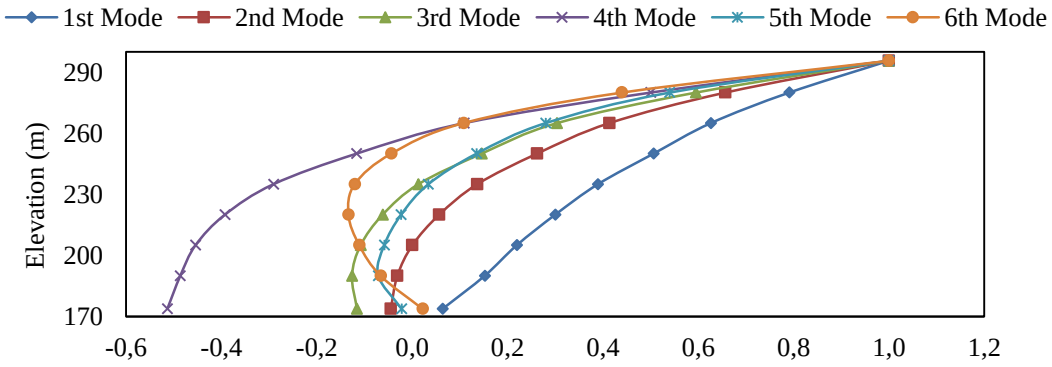

Figure 6: Normalized mode shapes at line (A-C) for WRWL

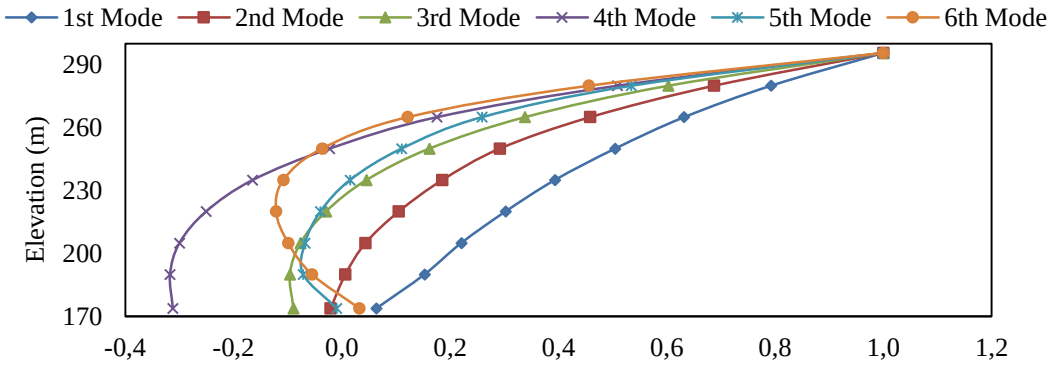

Figure 7: Normalized mode shapes at line (A-C) for SRWL

3.2 Case B

Case B deals with the foundation block only, which is a reduced-domain for a uniform half-space. The loading condition is a vertically-propagating SH wave, induced by a shear-stress time-history provided for input to the base of the foundation. As a consequence, each element column behaves exactly as the adjacent one (uniaxial problem) and the time histories at the surface have to be the same. Analyzing an uniaxial problem is not the goal of this case. The goal of this case is to analyze the disturbance applied by the same boundary condition used in case C, D, E to the above mentioned solution. No damping was applied.

Since in this case the energy arrives from a far-field source through a vertically propagating SH wave (see [4]), the infinite elements have two functions: (a) allowing the incoming waves to penetrate in the near-field-domain, (b) not reflecting the outgoing waves generated by the scattered motion induced by the dam and reservoir (see [4]). In a first analysis we didn't apply any external force on the vertical viscous boundary.

The 36 time histories obtained by the authors (velocities at 9 points for two foundation length and two impulses) are shown in the final report prepared by the formulators.

Point a in Figure 8 is at the center of the foundation free surface. Its velocity response, to the given impulse, can be assumed as the undisturbed result. On the contrary, points c, e, g are at 100,20,0 m from the right boundary respectively. Therefore their velocity response is lower, because a fraction of energy is absorbed by the viscous vertical boundary. Figure 8 show the comparison between disturbed and undisturbed velocity, for cases B-1(high frequency,700 m length), B-2(low frequency,700 m length), B-3(high frequency, 3700 m length), B-4(low frequency, 3700 m length). The difference observed is due to the fact that we had not enough time to implement a boundary condition on the vertical sides which is compliant with the free-field solution.

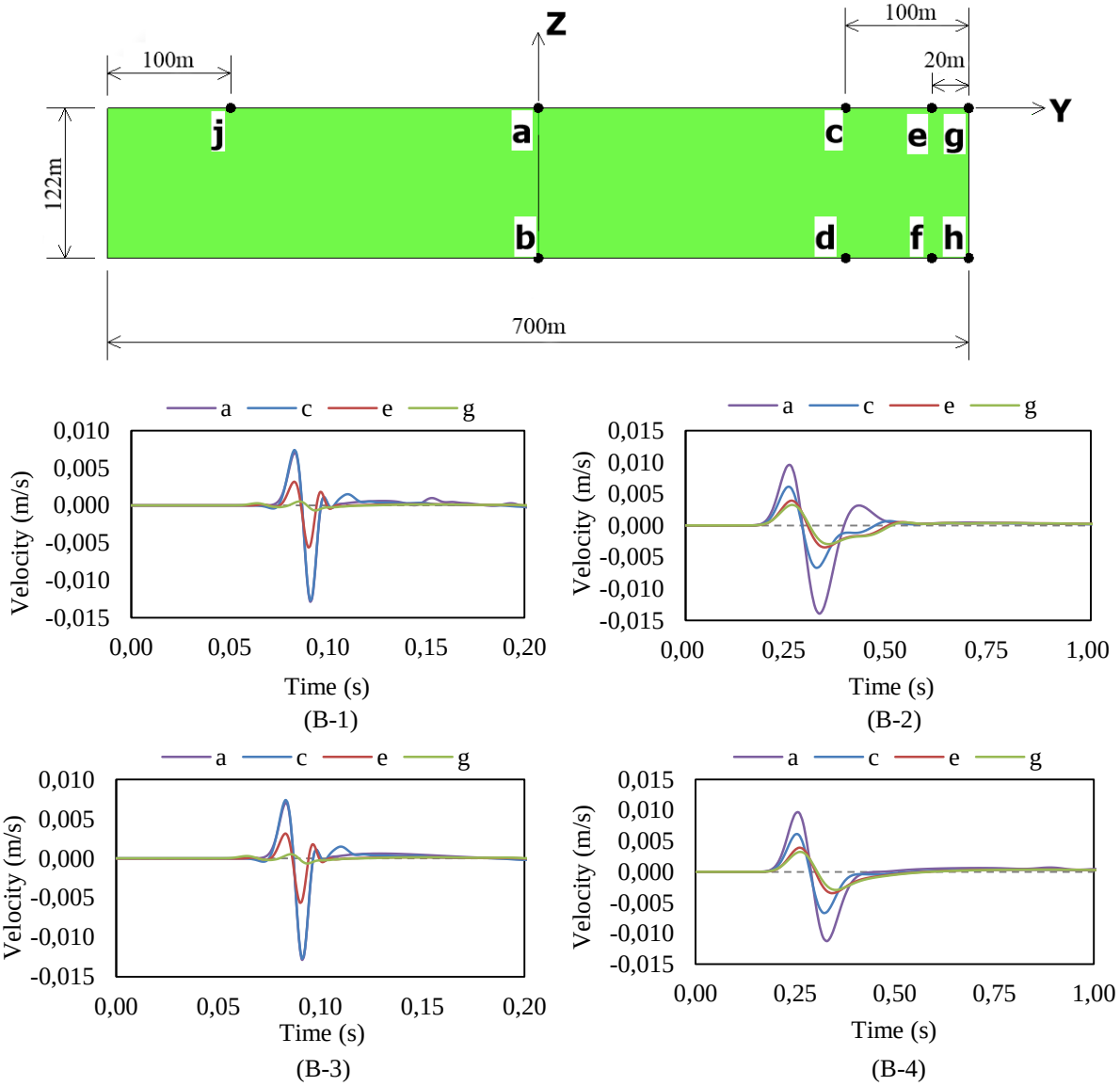

Figure 8: Velocities response time histories at point (a) , point (c), point (e), and point (g)

3.3 Case C

The analysis type for Case C is related to the one conducted for Case B-1 and B-2. Here, the dam and the reservoir are considered together with the foundation model. Figure 9 shows the results for high frequency signal, with (subscript 1) and without (subscript 3) reservoir. Figure 10 shows the results for low frequency signal, with (subscript 2) and without (subscript 4)

reservoir. The purpose of the study for Case C is to investigate the effect of the dam and reservoir presence on the wave propagation in the foundation and to compare the analysis results with the free field motions studied in Case B. No damping was applied.

Points a, c, e are in the same position as in the previous case B. At point c, reverberations after the main pulse are produced primarily by the interaction of the dam and reservoir.

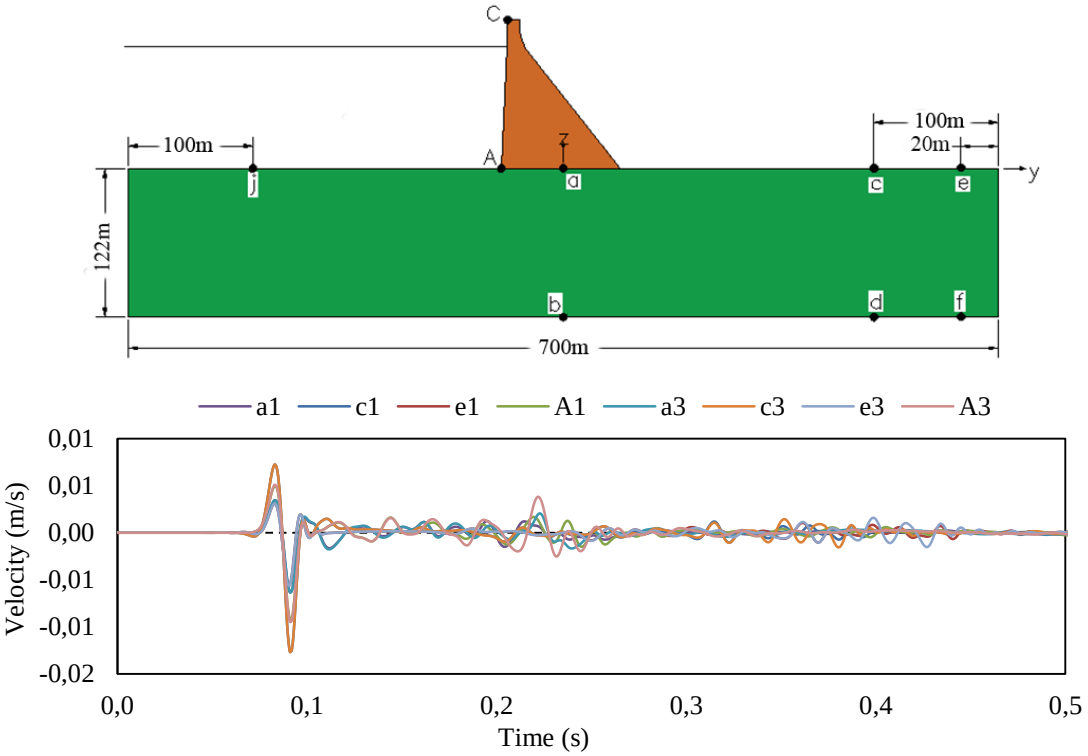

Figure 9: Velocities response time histories at different points (high frequency)

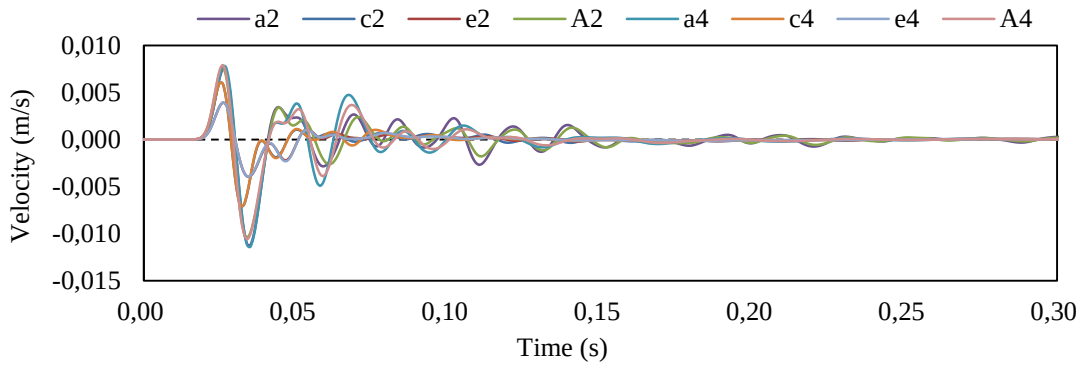

Figure 10: Velocities response time histories at different points (low frequency)

3.4 Case D

In Case D, a dynamic analysis of the dam-foundation-reservoir system is performed considering the elastic material properties, the Taft earthquake record, and the reservoir water at two different elevations. More precisely, the deconvolved stress time history was applied at the base of the foundation block. The intent is to evaluate the dam response due to various reservoir levels.

Figure 11 shows the history of hydrodynamic pressure at heel [point A]. Figure 12 and Figure 13 show the history of acceleration at heel [point A] and crest [point C]. The differences between the two diagrams are very small.

The acceleration time history computed at point A approximately match the free-surface Taft record, and the time history computed at point C is substantially larger.

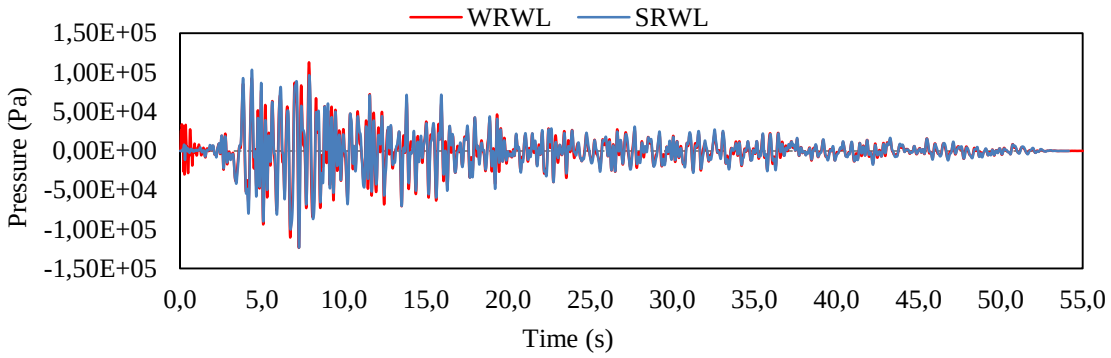

Figure 11: History of hydrodynamic pressure at heel [point A] for WRWL and SRWL

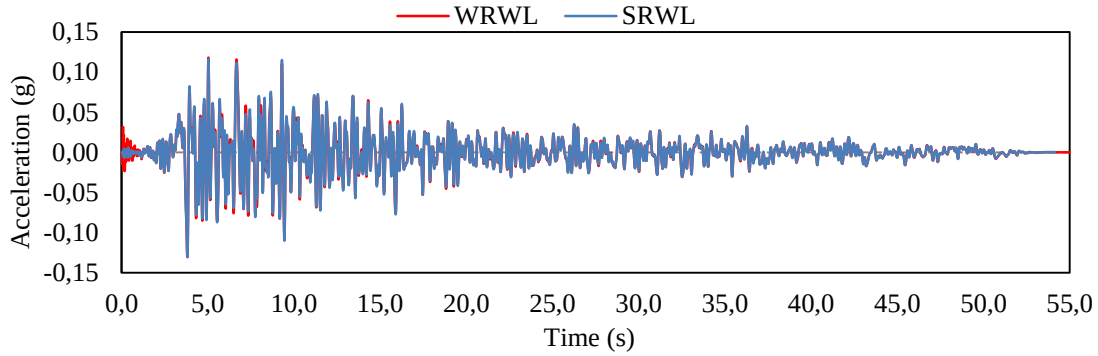

Figure 12: History of acceleration at heel [point A] for WRWL and SRWL

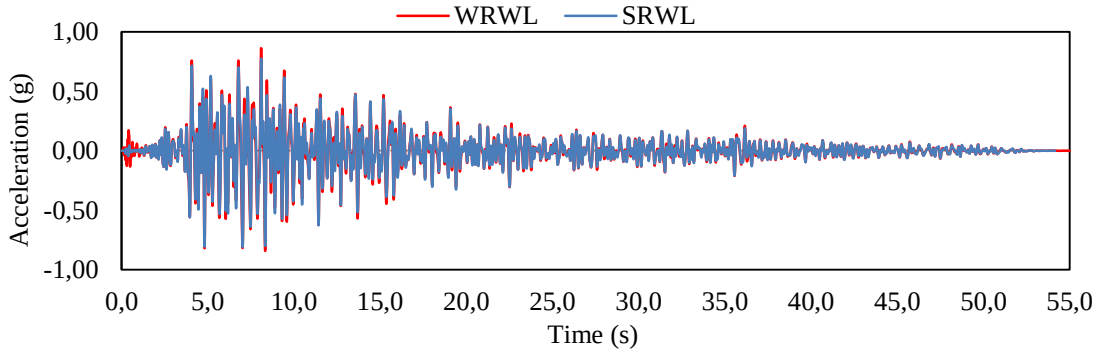

Figure 13: History of acceleration at crest [point C] for WRWL and SRWL

3.5 Case E

The intent of Case E is to perform a dynamic analysis with concrete non-linear material properties. The dam-foundation-reservoir system used in Case D will be analyzed except the non-linear material properties of concrete are considered. The concrete damaged plasticity model is used.

During the non-linear analysis, the compressive strength of 28 MPa (see Table 1) is never achieved. On the contrary, the tensile strength of 2 MPa is reached at point A (re-entrant corner at upstream side). The softening behavior of concrete, after the peak value, is assumed according to [5] (see Figure 14). It is assumed that the softening process occurs in a narrow band of thickness equal to one element (crack-band=1.48m), while the elements outside this band unload elastically. This assumption allow us to transform the critical value of displacement discontinuity w_c, computed according to [5] and the fracture energy given by the formulators,

into the critical value of the cracking strain $(\epsilon_c)_c$ =(w_c /crack-band) required by the concrete damaged plasticity model. With comparison to the length of the dam-foundation joint (95.8 m), this hypothesis corresponds to the formation of a cohesive crack. It is well known that the softening behaviour can induce convergence problems, due to the bifurcation of the equilibrium path in the incremental solution process. These problems occur in quasi-static analysis (see [6],[7]), as well as in this dynamic implicit analysis. In order to overcome this problem: (a) the time history of the deconvolved acceleration was used as load; (b) a set of parameters, suggested by the Abaqus manual as 'application=moderate dissipation' was used.

The material behavior in unloading condition is characterized by a stiffness k_{unl} which depends on the damage index as follow: d = 1.0-k_{unl}/$k_{first\_loading.}$ The value of d is assumed as a piecewise linear function of ϵ_c. During the first loading phase, it is assumed d=0; just after the peak load, when the cracking strain ϵ_c starts to grow it is assumed d=0.25; at the knee point it is assumed d=0.78; when ϵ_c reach the critical value it is assumed d=1 and no stress transfer occurs.

In Case E, the tensile strength is achieved at the above mentioned re-entrant corner, for T_1 = 3.785 sec after the excitation beginning. This is the first damage occurring in the model. Afterwards the cohesive crack starts to propagate along the dam-foundation joint and the last damage occurs for T_2= 7.031 sec, at a distance of 16.5 m from the re-entrant corner.

Since an automatic time step dt is assumed, dt drops from 1.e-2 sec to 1.e-6 sec every time the peak stress is reached in a new, undamaged element.

According to the formulation document [1], the Rayleigh damping matrix is assumed as C = αM +βK, where M is the mass matrix, K is the stiffness matrix, α= 0.75 1/sec and β = 0.0005 sec. Since the Abaqus code does not propagate to the C matrix the reduction of stiffness induced by damage, on the safety side, for the first 15 concrete elements along the dam foundation joint, it was assumed β= 0.

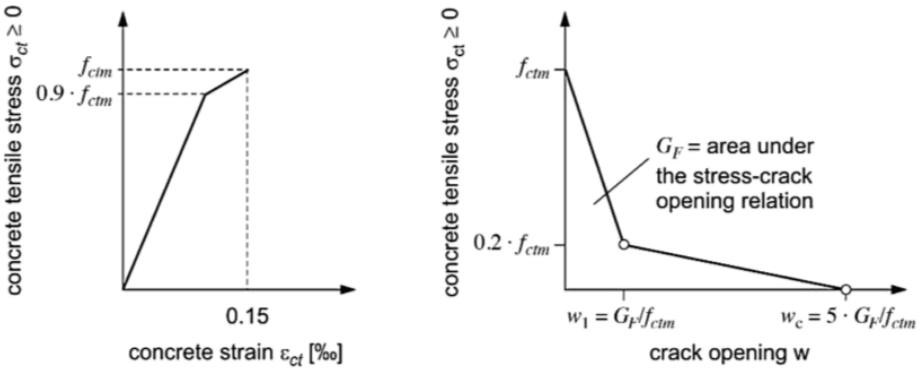

Figure 14: Schematic representation of the stress-strain and stress-crack opening relation for uniaxial tension, according to [5]

For case E only, in order to simulate the free-field motion on both vertical sides of the foundation, a two-step-procedure was used:

In a first model B analysis, without dam and reservoir, the condition U2=0 was applied on both vertical sides. In this model all points in the foundation surface move in the same way. Both the histories of the related reaction force RF2 and the histories of the displacement U1 were recorded.

In a second model, the condition U2=0 was removed and the histories RF2 were applied. Furthermore the viscous boundary elements were added on the vertical sides and the necessary forces to impose the previously recorded histories U1 were imposed, as well.

A specific python code was written in order to manage the above mentioned histories.

Since the application of this procedure to case B was successful, it was repeated in the case E.

Table 1. Concrete properties and parameters applied in the Abaqus code

Parameters	**values**	**Parameters**	**values**
Modulus of elasticity	22410MPa	Tensile strain at peak load	0.00012
Density	2483kg/m^3	Dilation angle	30°
Poisson's ratio	0.20	Eccentricity	0.1
Compressive strength	28.0MPa	f_{b0}/f_{c0}	1.16
Tensile strength	2.0MPa	*K*	0.6666
Fracture energy	250N/m	Viscosity parameter	0.0
Compressive strain at peak load	0.0025		

Note: (1)f_{b0}/f_{c0} is the ratio of initial equibiaxial compressive yield stress to initial uniaxial compressive yield stress.
(2)The eccentricity is a small positive number that defines the rate at which the hyperbolic flow potential approaches its asymptote.
(3) *K* is the ratio of the second stress invariant on the tensile meridian to that on the compressive meridian.

According to the formulation document: (a) viscous damping of 2% was applied to the dam and foundation; (b)the uplift pressure induced by the water penetrating the crack was not taken into account (see [8]).

Figures 15 and 16 show the acceleration response histories at heel [point A] and crest [point C] for WRWL respectively. Figure 17 show the history of hydrodynamic pressure at heel [point A].

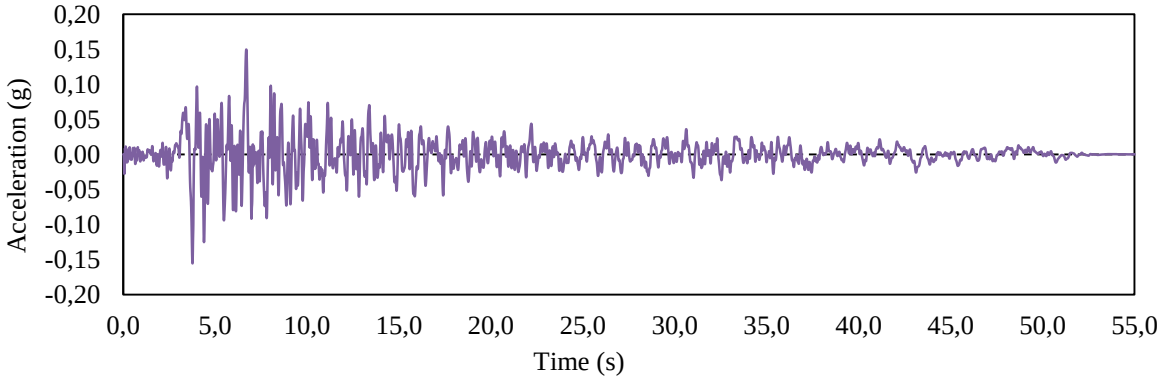

Figure 15: History of acceleration at heel [point A] for WRWL

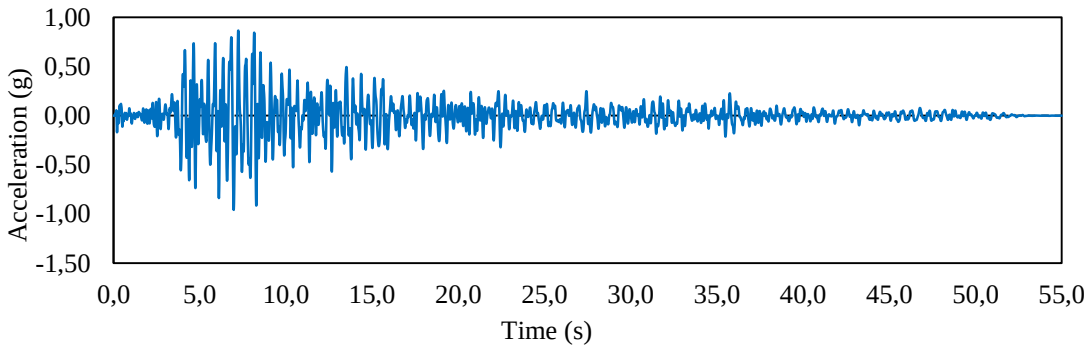

Figure 16: History of acceleration at crest [point C] for WRWL

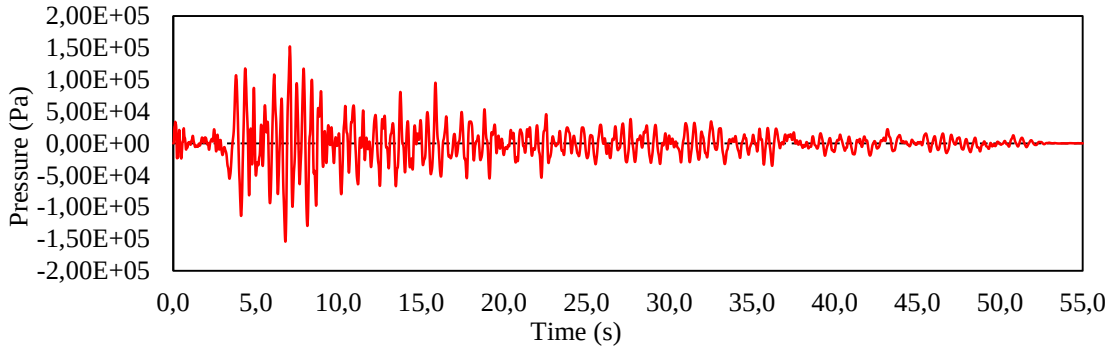

Figure 17: History of hydrodynamic pressure at heel [point A] for WRWL

4 Conclusions

-In case of a dynamic force applied to the near field, the viscous-boundary available in Abaqus code performs properly. No specific code is necessary.

-In case of vertical propagating SH-waves, a specific python code was necessary to model the free field motion on the vertical boundaries properly. This procedure was applied to case E only.

-The Taft records induces damage on the first 16.5 m of dam-foundation joint, over a total length of 98.5 m.

-The uplift pressure induced by the water penetrating the crack was not taken into account.

5 References

[1] J. Salamon et all. Theme a formulation: Seismic analysis of Pine Flat concrete dam. International Commission on Large Dams, 2019.

[2] Dassault. Systems. SIMULIA. Corp., editor. Abaqus 6.18 documentation. Johnston, RI 02919, USA, 2018.

[3] O. C. Zienkiewicz, R. L. Taylor. (2000). The Finite Element Method, 5td Edition, ISBN 13: 9780750650496.

[4] Wolf J.P., Dynamic soil-structure interaction, Prentice- Hall International Series in Civil Engineering and Engineering Mechanics, ISBN 0-13-221565-9,1988

[5] International. Federation. for. Structural. Concrete, editor. Model Code for Concrete Structures. Ernst & Sohn, a Wiley Brand, Berlin, Germany, 2010. ISBN:978-3-433-03061-5, www.b-international.org/b-model-code-2010.

[6] S. Valente. Bifurcation phenomena in cohesive crack propagation. Computers and Structures, 44(1/2):55-62, 1992.

[7] F. Barpi, S. Valente, M. Cravero, G. Iabichino, and C. Fidelibus. Fracture mechanics characterization of an anisotropic geoma-terial. Engineering Fracture Mechanics, 84:111-122, 2012. ISSN:0013-7944,doi:10.1016/ j.engfracmech. 2012.01.010.

[8] F. Barpi, S. Valente. Modeling water penetration at dam-foundation joint, Engineering Fracture Mechanics.75/3-4:629-642, doi 10.1016/j.engfracmech.2007.02.008